# Accepted Manuscript

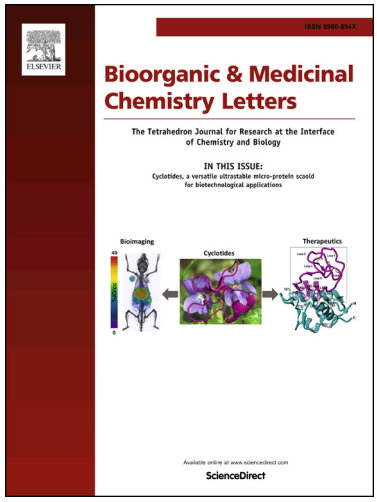


Spiro-1-benzofuranpiperidinylalkanoic acids as a novel and selective sphingosine $S1P_5$ receptor agonist chemotype

Axel R. Stoit, Jos H.M. Lange, Hein K.A.C. Coolen, Annemieke Rensink, Adri van den Hoogenband, Arnold P. den Hartog, Sjoerd van Schaik, Chris G. Kruse

PII: S0960-894X(17)31178-2
DOI: https://doi.org/10.1016/j.bmcl.2017.12.018
Reference: BMCL 25474

To appear in: *Bioorganic & Medicinal Chemistry Letters*

Received Date: 29 September 2017
Accepted Date: 8 December 2017

Please cite this article as: Stoit, A.R., Lange, J.H.M., Coolen, H.K.A., Rensink, A., van den Hoogenband, A., den Hartog, A.P., van Schaik, S., Kruse, C.G., Spiro-1-benzofuranpiperidinylalkanoic acids as a novel and selective sphingosine $S1P_5$ receptor agonist chemotype, *Bioorganic & Medicinal Chemistry Letters* (2017), doi: https://doi.org/10.1016/j.bmcl.2017.12.018

# Spiro-1-benzofuranpiperidinylalkanoic acids as a novel and selective sphingosine $S1P_5$ receptor agonist chemotype

Axel R. Stoit, Jos H. M. Lange*, Hein K. A. C. Coolen, Annemieke Rensink, Adri van den Hoogenband, Arnold P. den Hartog, Sjoerd van Schaik and Chris G. Kruse

Abbott Healthcare Products B.V. (formerly Solvay Pharmaceuticals B.V.), C. J. van Houtenlaan 36, 1381 CP Weesp, The Netherlands



* Direct correspondence to Dr. J.H.M. Lange, Kraton Chemical B.V., Transistorstraat 16, 1322 CE Almere, The Netherlands. Telephone: +31 (0)365462800. E-mail: jos.lange@kraton.com

**Abstract**. The synthesis and SAR of a novel class of spirobenzofuranpiperidinyl-derived alkanoic acids **6**-**34** as sphingosine $S1P_5$ receptor agonists are described. The target compounds generally elicit high $S1P_5$ receptor agonistic potencies and in general are selective against both $S1P_1$ and $S1P_3$ receptor subtypes. The key compound **32** shows a high bioavailability of 73% and a CNS/plasma ratio of 0.8 after oral administration in rats.

**Keywords**: $S1P_5$ Receptor agonists; Subtype selectivity; Spirocyclic scaffold; Molecular modelling; Homology model; Oral bioavailability; Turbidimetric aqueous solubility; Microsomal stability; Membrane permeation

Sphingosine-1-phosphate (S1P, **1**) is a bioactive lipid with important functions in multiple cellular signaling systems[1]. S1P affects the central nervous system,[2] cardiovascular system and immune system and has been implicated in a broad range of diseases[3] (Figure 1). S1P also activates the G protein-coupled sphingosine receptors $S1P_1$ - $S1P_5$. The approval of the S1P receptor agonist fingolimod (**2**, FTY720, Gilenya®) in 2010 for the treatment of relapsing multiple sclerosis has intensified sphingosine research efforts.[4] Compound **2** acts as a pro-drug by phosphorylation into the active (*S*)-Fingolimod-phosphate (**3**) which is an analogue of **1**. Compound **2** was reported[5] to act (*via* **3**) on four of the five S1P receptor subtypes (excluding $S1P_2$) and to lead to lymphopenia. More S1P receptor subtype selective ligands with better pharmacokinetic profiles and fewer side effects will be required[4,6] to further elucidate the physiological background and therapeutic roles of $S1P_{1-5}$. Several selective $S1P_{1/5}$ receptor dual agonists have been discovered such as siponimod, ozanimod, ceralifimod, AMG369[7] and GSK2018682 for the treatment of multiple sclerosis and other autoimmune and inflammatory disorders.[4,8]

The $S1P_5$ receptor is most highly expressed in the central nervous system, particularly on oligodendrocytes and brain endothelium. The $S1P_5$ receptor was shown to mediate the immune quiescence of the human endothelium barrier.[9] The number of orally available, selective $S1P_5$ receptor agonists is very limited. The 2*H*-phthalazin-1-one analogue **4** was reported[10] by Novartis as a selective and orally active $S1P_5$ receptor agonist. Recently, A-971432 was disclosed[11] as a highly selective $S1P_5$ receptor agonist. A-971432 exhibited excellent plasma and CNS exposure after oral dosing in several preclinical species and reversed lipid accumulation as well as age-related cognitive decline in rodents. Hanessian reported[12] the chiral pyrrolidine derivative **5** which acted as an agonist on both $S1P_4$ and $S1P_5$, being devoid of activity at $S1P_1$ and $S1P_3$. Compound **5** can be regarded as a

constrained azacyclic analogue of **3** and has a relatively poor pharmacokinetic profile. It serves in the present study as a molecular modeling tool.

Herein, a set of novel spirocyclic benzofuranpiperidinylalkanoic acids **6**-**34** and the phosphate analogue **35** are disclosed as a new selective $S1P_5$ receptor agonist chemotype.

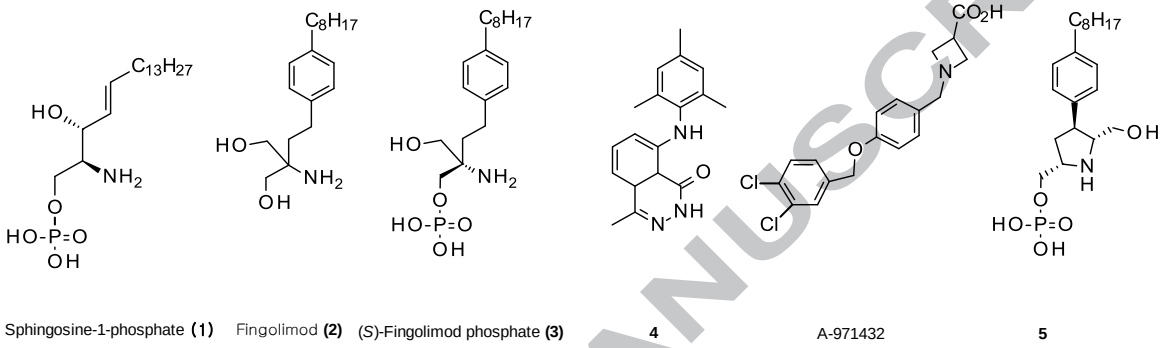


**Figure 1.** Chemical structures of selected S1P receptor agonists.

The synthesis of the target 2*H*-spiro(1-benzofuran-3,4'-piperidine) compounds **6**-**21** is depicted in Scheme 1. 2-Bromo-5-methoxyphenol **36** was coupled to the protected tetrahydropyridinemethanol derivative[13] **37** in a Mitsunobu reaction to give **38** in 63% yield. Radical spirocyclization of **38** in the presence of tributyltin hydride and a catalytic amount of the radical initiator AIBN provided **39** in a chemical yield of 68%. The methoxy group in **39** was removed under strongly acidic conditions to furnish **40** in quantitative yield. Reductive debenzylation of **40** efficiently led to **41** which was converted into **42** by reaction with *tert*-butylacrylate in the presence of diisopropylamine as organic base. Mitsunobu coupling of **42** with a set of appropriate alcohols gave the *tert*-butyl esters **43**-**58**, respectively. The target compounds **6**-**21** were obtained from **43**-**58** by acidic removal of their *tert*-butyl protective group, thereby liberating the carboxylic acid moiety.

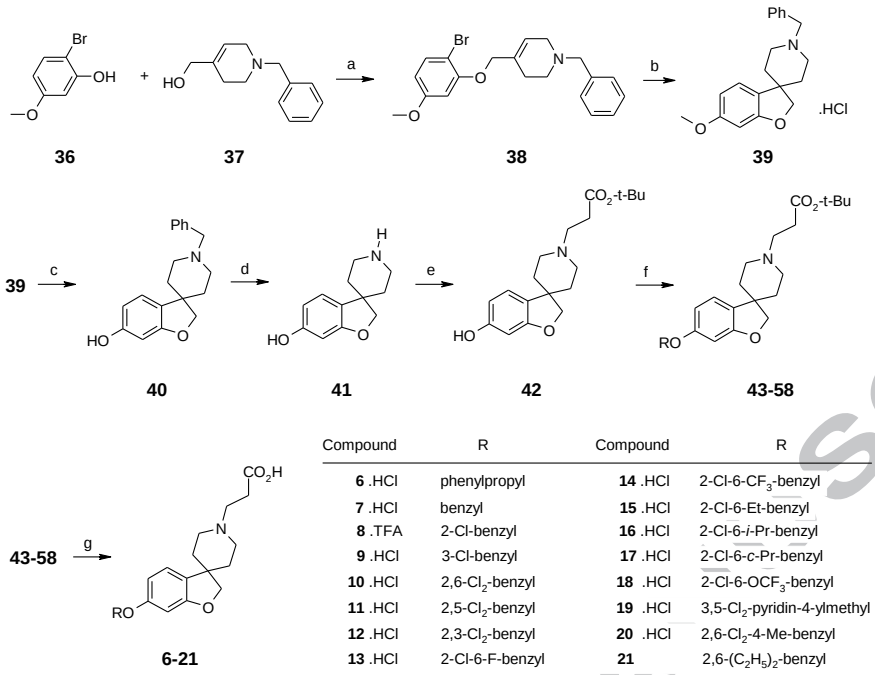


| Compound | R | Compound | R |
|---|---|---|---|
| **6** .HCl | phenylpropyl | **14** .HCl | 2-Cl-6-$CF_3$-benzyl |
| **7** .HCl | benzyl | **15** .HCl | 2-Cl-6-Et-benzyl |
| **8** .TFA | 2-Cl-benzyl | **16** .HCl | 2-Cl-6-*i*-Pr-benzyl |
| **9** .HCl | 3-Cl-benzyl | **17** .HCl | 2-Cl-6-*c*-Pr-benzyl |
| **10** .HCl | 2,6-$Cl_2$-benzyl | **18** .HCl | 2-Cl-6-$OCF_3$-benzyl |
| **11** .HCl | 2,5-$Cl_2$-benzyl | **19** .HCl | 3,5-$Cl_2$-pyridin-4-ylmethyl |
| **12** .HCl | 2,3-$Cl_2$-benzyl | **20** .HCl | 2,6-$Cl_2$-4-Me-benzyl |
| **13** .HCl | 2-Cl-6-F-benzyl | **21** | 2,6-$(C_2H_5)_2$-benzyl |




**Scheme 1.** Reagents and conditions: (a) $PPh_3$, DIAD, THF, < 10 $^oC$, 2h followed by rt, 16 h (63%). (b) *n*-$Bu_3SnH$, AIBN (cat.), benzene, $N_2$, reflux, 16 h (68%). (c) 48% HBr, AcOH, reflux, 24 h (quantitative yield). (d) $H_2$, $Pd(OH)_2$, 4N HCl, MeOH, rt, 48 h (68%). (e) *tert*-butylacrylate, $(i\text{-}Pr)_2NH$, MeOH, reflux, 16 h (91%). (f) R-OH, $PPh_3$, DIAD, $CH_2Cl_2$, rt, 16 h (50-90%). (g) 4M HCl, 1,4-dioxane, 50 $^oC$, 16 h (80-95%).

The synthesis of the fluoro analog **22** is depicted in Scheme 2. The aromatic difluoride[14] **59** was coupled to 4-pyridinemethanol **60** to furnish **61**. Benzylation of **61**, followed by partial reduction of the *in situ* formed positively charged quaternary pyridine ring by sodium borohydride in methanol at low temperature gave **62**. Microwave-assisted radical spirocyclization of **62** in the presence of tributyltin hydride and a catalytic amount of radical initiator provided **63** in a chemical yield of 72%. Subsequent reductive debenzylation by ammonium formate in the presence of $Pd(OH)_2$ gave a high yield of **64** which was analogously converted as described earlier for **6**-**21** to the fluorinated target compound **22** *via* the intermediates **65** and **66**.

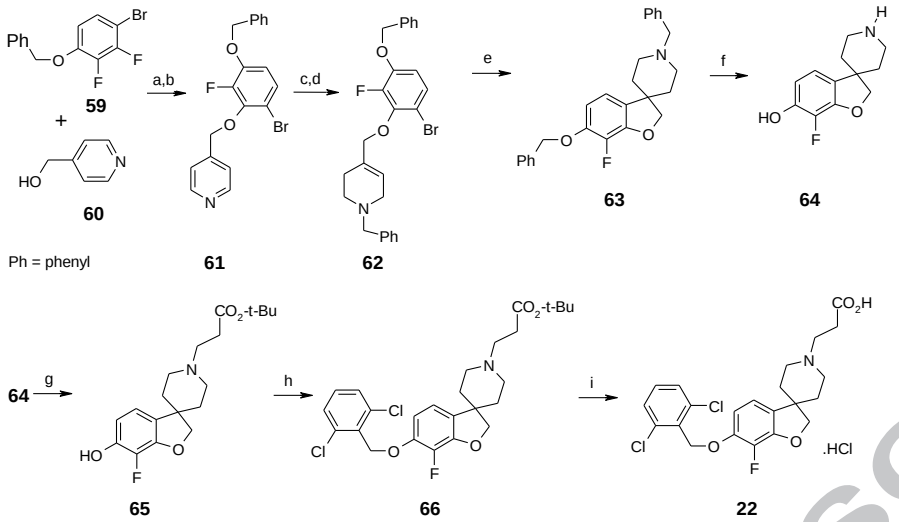


**Scheme 2.** Reagents and conditions: (a) reaction of **60** with NaH, NMP, rt, 30 min. (b) Addition of **59**, 100 $^{o}$C, 15 min (83%). (c) BnBr, acetone, 40 $^{o}$C, 16 h. (d) $NaBH_4$, MeOH, -10 $^{o}$C→rt, 4 h (63%). (e) n-$Bu_3SnH$, 2,2'-azobis(2-methylpropionitrile) (cat.), benzene, microwave, SiC, 175 $^{o}$C, 1 h (72%). (f) ammonium formate, $Pd(OH)_2$, MeOH, 60 $^{o}$C, 16 h (96%). (g) *tert*-butylacrylate, (i-$Pr)_2NH$, MeOH, reflux, 16 h (82%). (h) R-OH, $PPh_3$, DIAD, $CH_2Cl_2$, rt, 16 h (66%). (i) 4M HCl, 1,4-dioxane, 50 $^{o}$C, 16 h (85%).

The synthesis of the target compounds **23**-**26** with a modified carboxylic acid chain is shown in Scheme 3**.** The synthesis route proceeds analogously to the reaction sequence of scheme 1, *viz.* reaction of the spirocycle **41** with either a bromoalkylcarboxylic acid *tert*-butyl ester (leading to **67**-**68**) or *tert*-butylmethacrylate (leading to **69**) in the presence of a base, followed by a Mitsunobu coupling and acidic hydrolysis of the formed *tert*-butyl esters **70**-**72**, respectively, to afford **23**-**25**. The analogue **26** was made analogously to **25** by applying (2-chloro-6-ethylphenyl)methanol in the Mitsunobu reaction instead of (2,6-dichlorophenyl)methanol.

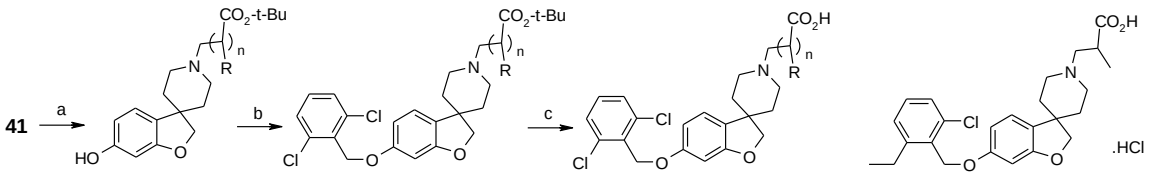

**Scheme 3.** Reagents and conditions: (a) for **23**: $BrCH_2CO_2$-*t*-Bu, DIPEA, $CH_3CN$, 65 °C 16 h (89 %); for **24**: $Br(CH_2)_3CO_2$-*t*-Bu, $K_2CO_3$, $CH_3CN$, 65 °C, 16 h (75 %); for **25**: $H_2C=C(CH_3)$-$CO_2$-*t*-Bu, DBU, DMF, 140 °C, 16 h, sealed flask (47 %). (b) 2,6-$Cl_2$-$C_6H_4CH_2OH$, $PPh_3$, DIAD, $CH_2Cl_2$, rt, 16 h (90-98 %). (c) 4M HCl, 1,4-dioxane, rt, 48 h (**23**: 86%, **24**: 87%, **25**: 80%).

The synthesis of the target compounds **27** and **28** is shown in Scheme 4**.** The phenolic hydroxy group of **42** was converted in its triflate **73**. A hetero cross coupling reaction between **73** and potassium thioacetate[15] mediated by $Pd_2(dba)_3$/CypF-*t*-Bu smoothly gave **74**. After liberation of the thiol group under mild basic conditions and coupling to the appropriate arylmethyl bromides, **75** and **76** were obtained, respectively. Acidic ester hydrolysis of **75** and **76** led to the target compounds **27** and **28**. Compound **75** was converted to the corresponding hydrochloride salt by brief treatment with 4M HCl in 1,4-dioxane and its sulfanyl moiety was subsequently oxidized by oxone into a sulfonyl group. Target compound **29** was obtained by acidic ester hydrolysis of **77**.

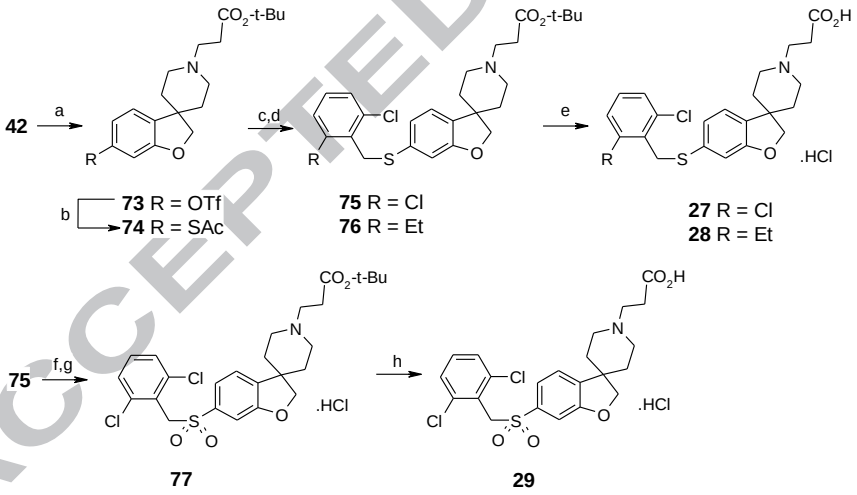


**Scheme 4.** Reagents and conditions: (a) Trifluoromethanesulfonimide, DMAP, $Et_3N$, $CHCl_3$, 60 °C, 16 h (93%). (b) KSAc, $Pd_2(dba)_3$, CyPF-*t*-Bu, toluene, 110 °C 24 h (80%). (c) NaOH pellets, EtOH, rt, 30 min. (d) 2-Cl-6-R-$C_6H_3$-$CH_2Br$, EtOH, 0 °C, 50 min (73%). (e) 4M HCl, 1,4-dioxane, rt, 48 h (87%). (f) 4M HCl, 1,4-dioxane, r.t., 5 min. (g) 3 Mol equiv. potassium peroxymonosulfate (Oxone), $H_2O$, rt, 2 h (72%). (h) 4M HCl, 1,4-dioxane, rt, 48 h (76%).

The synthesis of the target compounds **30**-**32** is depicted in Scheme 5**.** The Sonogashira[16] coupling of two arylacetylenes with the aryltriflate **73** gave **78** and **79**, respectively in high

yields. The alkynes **78** and **79** were hydrolyzed under acidic conditions to afford the target compounds **30** and **31**, respectively. The triflate moiety of **73** was successively converted into a tributylstannyl group (**80**) and bromo substituent (**81**). Subsequent treatment with the appropriate arylethenyl-$BF_3K$ reagent[17-19] in a toluene/water mixture at elevated temperature led to **82**, which was further hydrolyzed into target compound **32**.

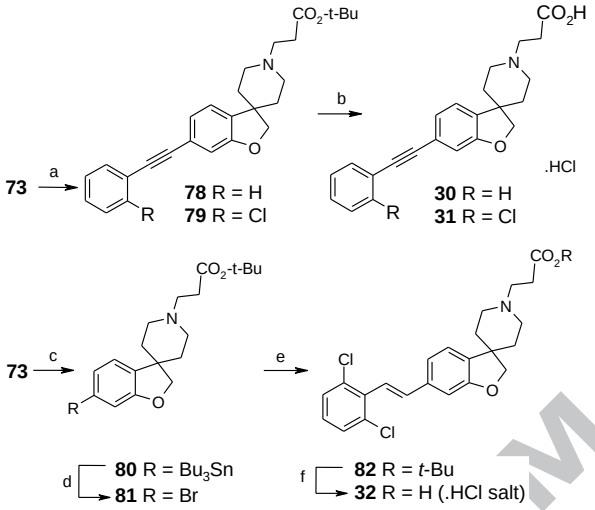


**Scheme 5.** Reagents and conditions: (a) 2-Cl-phenylacetylene or phenylacetylene, $Pd(OAc)_2$, $PPh_3$, $K_3PO_4.H_2O$, DMSO, 80 °C, 1 h (72-90%). (b) 4M HCl, 1,4-dioxane, 60 °C, 5 h (70-90%). (c) $Sn_2(n\text{-}Bu)_6$, $(PPh_3)_4Pd$, LiCl, 1,4-dioxane, 108 °C, 72 h (61%). (d) NBS, THF, 0 °C, 1.5 h (57%). (e) 2-[(E)-2-(2,6-$Cl_2$-$C_6H_3$)ethenyl]$BF_3K$, DPPF, $Cs_2CO_3$, toluene/water = 1/3, 100 °C, 16 h (67%). (f) 4M HCl, 1,4-dioxane, rt, 48 h (93%).

The 2*H*-spiro(1-benzofuran-3,3'-piperidine)-6-ol **83** was prepared in several steps analogously to the procedures described in scheme 2 by starting from 3-pyridinemethanol and 4-(benzyloxy)-1-bromo-2-fluorobenzene and was converted into **84** by reaction with *tert*-butylacrylate in the presence of a base. Mitsunobu coupling of **84** with two appropriate alcohols afforded **85** and **86**, respectively. These compounds were hydrolyzed into the target compounds **33** and **34**.

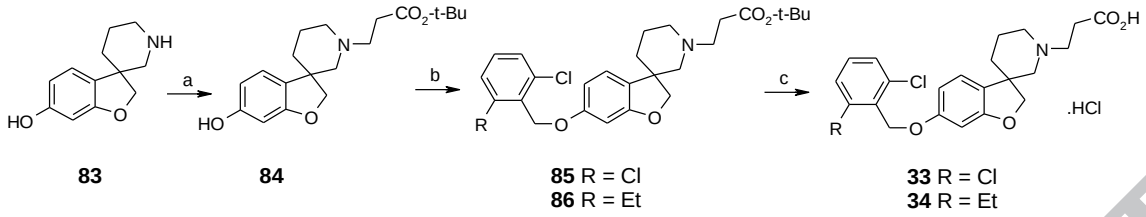


**Scheme 6.** Reagents and conditions: (a) *tert*-butylacrylate, $(i\text{-}Pr)_2NH$, MeOH, reflux, 16 h (84%). (b) $ArCH_2OH$, $PPh_3$, DIAD, $CH_2Cl_2$, rt, 16 h (**85**: 36%, **86**: 72%). (c) 4M HCl, 1,4-dioxane, 50 $^oC$, 2 h (73-82%).

The synthesis of the spirocyclic phosphate **35** is outlined in scheme 7. The key intermediate **41** was Boc-protected and the resulting **87** was O-benzylated in quantitative yield according to the Mitsunobu procedure into **88**. After Boc deprotection, the formed **89** was coupled with a THP-protected ethyloxy moiety to give **90**. THP-deprotection under acidic conditions led to the alcohol **91** which was isolated as its hydrochloride salt and subsequently reacted with di-*tert*-butyl *N*,*N*-diisopropylphosphoramidite, followed by treatment with *tert*-butylhydroperoxide to furnish the di-*tert*-butyl phosphonate **92**, which was hydrolyzed with mineral acid into the phosphate **35**.

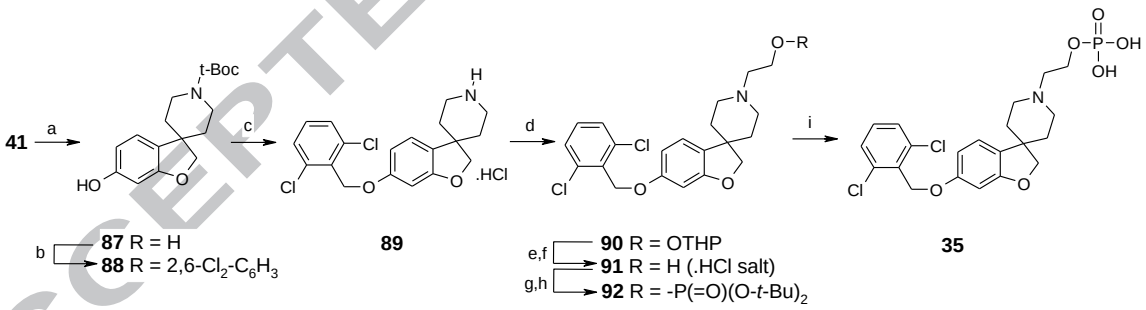


**Scheme 7.** Reagents and conditions: (a) $Boc_2O$, $CH_2Cl_2$, rt, 16 h (81%). (b) 2,6-$Cl_2$-$C_6H_3$-$CH_2OH$, $PPh_3$, DIAD, $CH_2Cl_2$, rt, 16 h (100%). (c) 1M HCl, EtOH, 50 $^oC$, 2 h (59%). (d) 2-(2-chloroethoxy)tetrahydro-2*H*-pyran, $K_2CO_3$, NaI (cat.), DMF, 100 $^oC$, 16 h (50%). (e) *p*-toluenesulfonic acid, MeOH, 50 $^oC$, 1 h. (f) 1M HCl, EtOH, rt, 1 h (8%). (g) di-*tert*-butyl *N*,*N*-diisopropylphosphoramidite, tetrazole, DMF/$CH_3CN$, rt, 2h. (h) *t*-BuOOH, nonane, rt, 30 min (62%). (i) 4N HCl, rt, 16 h (81%).

The pharmacological results of the pro-drug fingolimod (**2**) and the target compounds **6-35** are given in Table 1. They were primarily evaluated at the human $S1P_5$ receptor and also profiled at $hS1P_1$ and $hS1P_3$ receptor subtypes. Functional *in vitro* human S1P assays

were applied, based on aequorin-derived luminescence triggered by S1P receptor-mediated changes in intracellular calcium levels.

**Table 1.** Pharmacological *in vitro* results of fingolimod (**2**) and the target compounds **6-35**.

| Compound | $pEC_{50}$ ($S1P_5$),[a] | $pEC_{50}$ ($S1P_1$),[b] | $pEC_{50}$ ($S1P_3$),[c] | Compound | $pEC_{50}$ ($S1P_5$),[a] | $pEC_{50}$ ($S1P_1$),[b] | $pEC_{50}$ ($S1P_3$),[c] |
|---|---|---|---|---|---|---|---|
| **2** | 5.5 ± 0.2 | < 5.0[d] | 5.6 ± 0.5 | | | | |
| **6** | 5.7 ± 0.2 | 5.3 ± 0.1 | 5.8 ± 0.3 | **21** | 7.7 ± 0.1 | 5.8 ± 0.1 | 5.8 ± 0.1 |
| **7** | 6.0 ± 0.1 | < 4.5 | < 5.0 | **22** | 8.2 ± 0.2 | 6.0 ± 0.1 | < 5.0 |
| **8** | 6.9 ± 0.1[d] | n. d.[e] | < 4.5 | **23** | 7.5 ± 0.2 | 5.2 ± 0.1 | < 6.0 |
| **9** | 6.5 ± 0.1 | < 5.0 | < 5.0 | **24** | 7.8 ± 0.2 | 5.3 ± 0.1 | 5.9 ± 0.1 |
| **10** | 6.8 ± 0.2 | 5.2 ± 0.2 | < 5.0 | **25** | 7.2 ± 0.2 | 5.9 ± 0.1 | < 5.0 |
| **11** | 6.7 ± 0.2 | 4.9 ± 0.2[d] | 6.0 ± 0.2 | **26** | 7.8 ± 0.1 | 6.5 ± 0.1 | < 5.0 |
| **12** | 6.7 ± 0.2 | 5.8 ± 0.2 | < 5.0 | **27** | 7.9 ± 0.1 | < 5.0[d] | 5.4 ± 0.2[d] |
| **13** | 7.2 ± 0.2 | 5.2 ± 0.1 | < 5.0 | **28** | 8.6 ± 0.1 | 6.9 ± 0.1 | < 6.0 |
| **14** | 6.9 ± 0.2 | 6.5 ± 0.2 | < 5.0 | **29** | 6.1 ± 0.1 | < 4.5 | < 5.0 |
| **15** | 7.8 ± 0.1 | n. d.[e] | < 5.0 | **30** | 7.4 ± 0.2 | < 4.5 | < 5.0 |
| **16** | 7.6 ± 0.1 | 5.9 ± 0.1 | < 5.0 | **31** | 7.6 ± 0.2 | < 4.5 | < 5.0 |
| **17** | 7.8 ± 0.1 | 5.7 ± 0.1 | 5.7 ± 0.1 | **32** | 7.9 ± 0.1 | < 4.5 | < 5.0 |
| **18** | 7.7 ± 0.1 | 5.4 ± 0.1 | < 5.0 | **33** | 7.0 ± 0.1 | < 4.5 | < 5.0 |
| **19** | 6.5 ± 0.2 | < 4.5 | < 5.0 | **34** | 7.5 ± 0.1 | < 4.5 | < 5.0 |
| **20** | 8.1 ± 0.3 | 6.5 ± 0.1 | < 5.0 | **35** | 7.7 ± 0.1 | 6.6 ± 0.1 | < 5.0 |

[a]Agonism at the human $S1P_5$ receptor (stably transfected in CHO cells, Aequorin luminescence read-out), expressed as $pEC_{50}$ ± SEM values. The values represent the mean result based on at least three independent experiments, unless otherwise noted. [b]Agonism at the $S1P_1$ receptor (stably transfected in CHO cells, Aequorin luminescence read-out), expressed as $pEC_{50}$ ± SEM values. [c]Agonism at the $S1P_3$ receptor (stably

transfected in CHO cells, Aequorin luminescence read-out), expressed as $pEC_{50}$ ± SEM values. [d]Result of duplicate measurement. [e]n. d.: Not determined.

In general, compounds **6**-**34** can be regarded as rigidified analogs of the S1P receptor agonists **1** and **3**, wherein the polar phosphate group is replaced by a relatively less polar carboxylic acid moiety. A-971432 also complies with this general S1P agonist pharmacophore, thereby deviating from **4**, which is lacking a polar phosphate or carboxylic acid moiety. In this context, our spirocyclic phosphate derivative **35** constitutes a spirocyclic analog of **1** wherein the polar phosphate group is retained, like in Hanessian's rigidified molecular probe **5**.

The flexible phenylpropoxy analog **6** showed comparable $S1P_5$ receptor agonist potency as compared to the pro-drug fingolimod (**2**), but lacked selectivity against the $S1P_1$ and $S1P_3$ receptor subtypes. Replacement of the phenylpropoxy group in **6** by the smaller and less flexible benzyloxy group (**7**) led to retained $S1P_5$ receptor agonism in combination with $S1P_1$ and $S1P_3$ selectivity. This fortuitous finding prompted substitution efforts at the phenyl moiety of the benzyloxy group of **7** in order to increase the $S1P_5$ receptor agonist potency in this series. The incorporation of a 2-chloro substituent (**8**) increased the $S1P_5$ potency almost tenfold and turned out to be preferable over 3-Cl substitution (**9**). The related dichlorophenyl substituted analogs **10**-**12** did not lead to increased $S1P_5$ agonism. Replacement of one of the chloro atoms in **10** by a fluoro atom (**13**) or a $CF_3$ moiety (**14**) gave only small effects on $S1P_5$ agonism. However, a significant improvement on $S1P_5$ agonism was observed for the substitution by an ethyl group (**15**: $pEC_{50} = 7.8 \pm 0.1$). Alternative replacements of one of the chloro atoms in **10** by an isopropyl- (**16**), cyclopropyl- (**17**), or -$OCF_3$ group (**18**) led to increased $S1P_5$ agonistic potency but a phenyl (**10**) to pyridyl (**19**) ring modification had not much impact. The presence of an additional 4-methyl group (**20**) led to an approximate tenfold increase in $S1P_5$ receptor

agonism. The 2,6-diethylphenyl substitution pattern (**21**) was also well-tolerated by the $S1P_5$ receptor. Interestingly, the presence of an addition fluoro substituent in the central aromatic region (**22**) resulted in improved $S1P_5$ receptor agonism ($pEC_{50} = 8.2 \pm 0.2$).

In the compounds **23**-**26** the SAR of the terminal alkylcarboxylic acid chain was investigated in more detail. Interestingly, both truncation (**23**) and elongation (**24**) of the chain led to increased $S1P_5$ receptor agonism, whereas branching of the chain (**25** and **26**) had not much impact.

Replacement of the phenolic oxygen atom in **10** and **21** by a sulphur atom (**27** and **28**) led in both cases to improved $S1P_5$ receptor agonism, thereby rendering **28** ($pEC_{50} = 8.6 \pm 0.1$) as the most potent $S1P_5$ receptor agonist in our series. Contrarily, the corresponding more polar sulfonyl derivative **29** was almost 100 times less potent at this lipophilic GPCR. The arylethynyl congeners **30** and **31** were significantly more potent than their arylmethoxy counterparts **7** and **8**, respectively. The arylethenyl variant **32** ($pEC_{50} = 7.9 \pm 0.1$) was tenfold more $S1P_5$ agonistic than its arylmethoxy analogue **10**. Interestingly, the phospate **35** was found almost tenfold more $S1P_5$ agonistic than its carboxylic acid counterpart **10**.

The regioisomeric congeners **33** and **34** of **10** and **21**, respectively showed high $S1P_5$ receptor agonism. Interestingly, **34** elicited considerable higher selectivity over the $S1P_5$ and $S1P_5$ receptor subtypes than **21**.

From Table 1 it becomes clear that fingolimod (**2**) has no $S1P_5/S1P_3$ receptor selectivity in contrast with our more rigid spirocyclic series, apart from the more flexible phenylpropoxy analogue **6**. The majority of our target compounds elicited high $S1P_5/S1P_3$ receptor subtype selectivities. In particular, **20** and **22** elicited over 1000-fold $S1P_5/S1P_3$ selectivities, whereas **13**, **15**-**18, 23**, **25**-**28**, and **30**-**35** were found over 100-fold $S1P_5/S1P_3$ selective.

The target compounds **6-35** were also $S1P_5/S1P_1$ selective to varying degrees. In particular, compounds **27**, **30**, **31**, **32,** and **34** are of interest since they were found approximately 1000 fold $S1P_5/S1P_1$ selective.

The key compound **32** was also tested for agonism at the human $S1P_2$ and $S1P_4$ receptors. The compound was devoid of $S1P_2$ agonism ($pEC_{50} < 5.0$), but acted as an agonist at the $S1P_4$ receptor ($pEC_{50} = 7.1 \pm 0.1$).

**Table 2.** Turbidimetric aqueous solubility data and *in vitro* human microsomal stability data of fingolimod (**2**) and representative target compounds.

| Compound | Aqueous Solubility[a] | Microsomal stability[b] ($Cl_{int}$) | Microsomal stability[c] ($t_{½}$) | Compound | Aqueous Solubility[a] | Microsomal stability[b] ($Cl_{int}$) | Microsomal stability[c] ($t_{½}$) |
|---|---|---|---|---|---|---|---|
| **2** | 1/6.5 | n. d.[d] | n. d.[c] | **26** | 100/> 100 | 6.1 | 228 |
| **8** | 30/> 100 | 9.1 | 153 | **27** | 100/> 100 | 21 | 65 |
| **10** | 100/> 100 | 3.1 | 447 | **28** | 30/ 100 | 42 | 33 |
| **13** | 30/> 100 | 2.7 | 505 | **29** | 100/> 100 | 33 | 129 |
| **16** | 30/100 | 2.1 | 671 | **30** | 100/100 | 8.3 | 167 |
| **19** | > 100/> 100 | 13.9 | 100 | **32** | 30/ >100 | 0.76 | 1820 |
| **21** | 100/> 100 | 0.92 | 1510 | **33** | 100/> 100 | 3.1 | 454 |
| **22** | 30/100 | 6.5 | 213 | **34** | 100/> 100 | 3.4 | 409 |

[a]Kinetic (turbidimetric) solubility, determined at Cyprotex, expressed as the minimal/ maximal value in µM. [b] Human microsomal stability at $10^{-6}$ M, determined at Cyprotex, expressed as the intrinsic clearance ($Cl_{int}$) in µl/min/mg protein. [c]Human microsomal stability at $10^{-6}$ M, determined at Cyprotex, expressed as the half-life ($t_{½}$), in minutes. [d]n. d.: Not determined.

The aqueous solubility of a compound constitutes an important factor in determining its absorption from the gastrointestinal tract and ultimately its oral bioavailability. The turbidimetric solubility of fifteen representative target compounds was determined and

compared with fingolimod (**2**). The turbidimetric solubility of **2** was only modest. Contrarily, all tested target compounds exhibited much higher values (Table 2). This was according to our expectation since the presence of the ionisable nitrogen atom and carboxylic acid moiety in our target compounds are important features to ameliorate aqueous solubility.

Human microsomal stability studies were conducted to determine the *in vitro* intrinsic clearance and half-life of the fifteen target compounds. In general, the compounds were metabolically stable *in vitro*, with the exception of **19** and **27**-**29**. The presence of the metabolically vulnerable pyridyl ring in **19** and the sulphur atom in **27** and **28** may account for their reduced *in vitro* metabolic stability. The compounds **21** and **32** were found the most stable in this assay.

Since the Caco-2 permeability assay is an established method[20] to predict human intestinal permeability and to investigate drug efflux phenomena, fingolimod (**2**) and the target compounds **10**, **13** and **19** were tested herein. All three compounds showed satisfactory apparent permeability coefficient values ($P_{app}$(A-B)) which ranged from to 9-21 x $10^{-6}$ cm/s. On the contrary, the observed ($P_{app}$(A-B)) value for **2** was only 0.53 x $10^{-6}$ cm/s, which is an indicator for poor intestinal epithelial cell permeability. Interestingly, compound **2** appeared to be subject of active transmembrane transport processes since the observed Asymmetry Index (AI = $P_{app}$(B-A)/$P_{app}$(A-B)) value was 4.1. The AI values of **10** and **13** were 1.0 and 0.7, respectively which indicates that active transport is not a dominant factor. On the contrary, the more polar pyridyl congener **19** showed a higher AI value of 2.7.

In agreement with its favourable turbidimetric aqueous solubility and microsomal metabolic stability, the key compound **32** showed a good oral bioavailability (73%) in rat

after oral administration and also elicited a favourable CNS/plasma ratio of 0.8, which turned out to be significantly higher than the CNS/plasma ratio of its analogue **10** (0.2).

Homology models for the $S1P_1$ and $S1P_5$ receptors were built using the RCSB Protein Data Bank crystal structure at atomic resolution of 2.2 Å of bovine rhodopsin[21] (1U19). Compound **3** was manually docked into the $S1P_1$ receptor in a comparable way as reported earlier.[22] An important difference is the adaptation of the rotameric state of W6.48 (Trp268) to the *trans*-configuration, which is thought to be associated with the agonistic state of the receptor.[23-25] Compound **3** is bound via a double salt bridge with its basic nitrogen atom and phosphate group to the vicinal Glu-Arg couple on helix 3. The aromatic core has multiple π–π-stacking interactions with a cluster of aromatic residues. The tail is situated in a deep lipophilic pocket between helix 5 and 6 which is characteristic[26] for the GPCR lipid receptor cluster (CB, LPA and S1P).

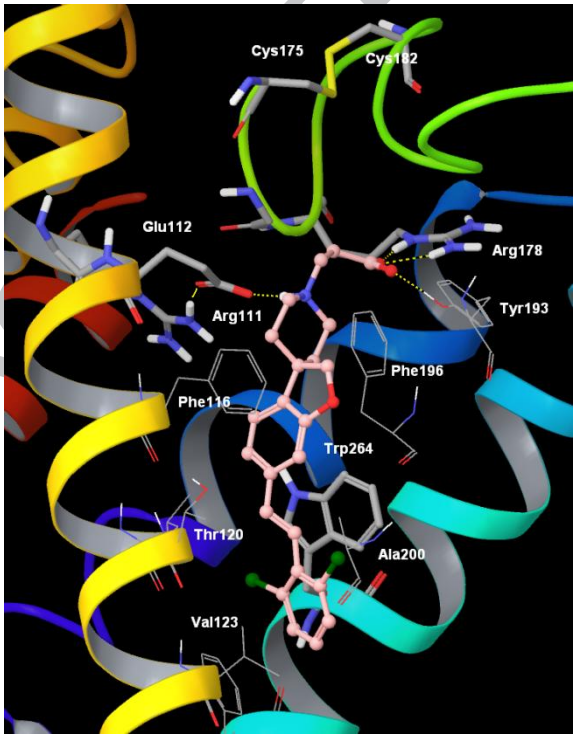


**Figure 2.** Compound **32** docked in the homology model of the $S1P_5$ receptor.

The binding pockets of the S1P-receptors are highly conserved. The marginal differences in interacting residues between the $S1P_1$ and $S1P_5$ receptors cannot account for the selectivity as observed for compound **5**. Significant dissimilarities, however, are found in the second extracellular loop. Especially of interest is the presence of an additional Arg in de EC2-loop of the $S1P_5$ receptor. In addition, it appeared not to be possible to dock **5** in the same way as compound **3**, having a double salt bridge with the Arg-Glu couple on helix 3. Due to the rigid configuration of the substituents on the chiral pyrrolidine ring, the phosphate group points towards the loop region. Therefore, it was hypothesized that the phosphate group of **5** interacts in the $S1P_5$ receptor with Arg178 and its protonated basic nitrogen with Glu112, which on itself is also bridged to Arg111. To this purpose the EC2-loop of our $S1P_5$-model was remodelled in such a way that Arg178 could have an optimal interaction with the phosphate group of **5**. Figure 2 shows a similar docking pose for compound **32** in our modified $S1P_5$ model. Besides an identical salt bridge pattern as described above, the benzofuran ring is stacked via several π–π-interactions with Trp264, Phe196 and Phe116, respectively. The 2-(2,6-dichlorophenyl)ethenyl-tail is positioned in a lipophilic pocket delimited by the Val123, Leu126, Ala200, Gly203, Ile204, Leu205, Ile208, Val256, Leu257, Val261 and Leu271 residues.

In conclusion, a new spirocyclic chemotype is disclosed which elicited high $S1P_5$ receptor agonistic potencies and showed varying degrees of both $S1P_1$ and $S1P_3$ receptor subtype selectivities. In general, the target compounds featured high turbidimetric aqueous solubilities as well as high *in vitro* human microsomal stabilities and membrane permeation. The potent and selective key compound **32** was found orally available (73%) in rat after oral administration in combination with a favourable CNS/plasma ratio of 0.8.

## Supporting information available

Selected analytical and synthetic data for compound **32**.

## References and notes


1. Marsolais D, Rosen H. *Nat Rev Drug Discov*. 2009;8:297-307.
2. Dev KK, Mullershausen F, Mattes H, Kuhn RR, Bilbe G, Hoyer D, Mir A. *Pharmacol Ther*. 2008; 117:77-93.
3. Kunkel GT, Maceyka M, Milstien S, Spiegel S. *Nat Rev Drug Discov*. 2013;12:688-702.
4. Park S, Im D. *Biomol Ther*. 2017;25:80-90.
5. Brinkmann V, Davis MD, Heise CE, Albert R, Cottens S, Hof R, Bruns C, Prieschl E, Baumruker T, Hiestand P, Foster CA, Zollinger M, Lynch KR. *J Biol Chem.* 2002;277:21453-21457.
6. Chew WS, Wang W, Herr DR. *Pharmacol Res.* 2016;113:521-532.
7. Cee VJ, Frohn M, Lanman BA, Golden J, Muller K, Neira S, Pickrell A, Arnett H, Buys J, Gore A, Fiorino M, Horner M, Itano A, Lee MR, McElvain M, Middleton S, Schrag M, Rivenzon-Segal D, Vargas HM, Xu H, Xu Y, Zhang X, Siu J, Wong M, Bürli RW. *ACS Med Chem Lett.* 2011;2:107-112.
8. O'Sullivan C, Schubart A, Mir AK, Dev KK. *J Neuroinflammation.* 2016;13:31.
9. Van Doorn R, Lopes Pinheiro MA, Kooij G, Lakeman K, van het Hof B, van der Pol SMA, Geerts D, van Horssen J, van der Valk P, van der Kam E, Ronken E, Reijerkerk A, de Vries HE. *J Neuroinflammation.* 2012;9:133.
10. Mattes H, Dev KK, Bouhelal R, Barske C, Gasparini F, Guerini D, Mir AK, Orain D, Osinde M, Picard A, Dubois C, Tasdelen E, Haessig S. *ChemMedChem*. 2010;5:1693-1696.
11. Hobson A, Harris C, van der Kam E, Turner S, Abibi A, Aguirre A, Bousquet P, Kebede T, Konopacki D, Gintant G, Kim Y, Larson K, Maull J, Moore N, Shi D, Shrestha A, Tang X, Zhang P, Sarris K. *J Med Chem.* 2015;58:9154−9170.
12. Hanessian S, Charron G, Billich A, Guerini D. *Bioorg Med Chem Lett.* 2007;17:491-494.
13. Gijsen HJM, De Cleyn MJA, Love CJ, Surkyn M, Van Brand SFA, Verdonck MGC, Moens L, Cuypers J, Bosmans JRMA. *Tetrahedron.* 2008;64:2456-2464.
14. Stensrud KF, Heger D, Sebej P, Wirz J, Givens RS. *Photochem Photobiol Sci.* 2008;7:614-624.

15. Van den Hoogenband A, Lange JHM, Bronger RPJ, Stoit AR, Terpstra JW. *Tetrahedron Lett.* 2010;51:6877-6881.

16. Chinchilla R, Nájera C. *Chem Rev.* 2007;107:874-922.

17. Darses S, Genet JP. *Chem Rev.* 2008;108:288-325.

18. Willis MC, Brace GN, Findlay TJK, Holmes IP. *Adv Synth Catal*. 2006;348:851-856.

19. Molander GA, Bernardi CR. *J Org Chem.* 2002;67:8424-8429.

20. Van de Waterbeemd H, Smith DA, Beaumont K, Walker DK. *J Med Chem*. 2001;44:1313-1333.

21. Okada T, Sugihara M, Bondar AN, Elstner M, Entel P, Buss V. *J Mol Biol.* 2004;342:571-583.

22. Pham TT, Fells JI, Osborne DA, North EJ, Naor MM, Parrill AL. *J Mol Graph Model.* 2008;26:1189-1201.

23. Ruprecht JJ, Mielke T, Vogel R, Villa C, Schertler GFX. *EMBO Journal*. 2004;23:3609-3620.

24. Pardo L, Deupi X, Govaerts C, Campillo M. 3-D Structure of G Protein-Coupled Receptors. In: Rognan D. ed. *Ligand Design for G Protein-Coupled Receptors.* Weinheim, Germany: Wiley-VCH; 2006, 183-203.

25. Jongejan A, Bruysters M, Ballesteros JA, Haaksma E, Bakker RA, Pardo L, Leurs R. *Nature Chem Biol.* 2005;1:98-103.

26. Surgand J, Rodrigo J, Kellenberger E, Rognan D. *Proteins.* 2006;62:509-538.

**Spiro-1-benzofuranpiperidinylalkanoic acids as a novel and selective sphingosine $S1P_5$ receptor agonist chemotype**

Axel R. Stoit, Jos H. M. Lange*, Hein K. A. C. Coolen, Annemieke Rensink, Adri van den Hoogenband, Arnold P. den Hartog, Sjoerd van Schaik and Chris G. Kruse

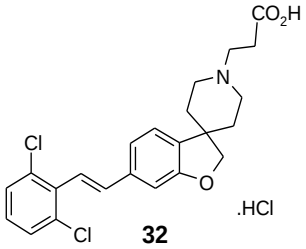


**32**

The potent and orally available $S1P_5$ receptor agonist **32** showed high $S1P_5$ receptor selectivities against the $S1P_{1-3}$ receptor subtypes.

* Direct correspondence to Dr. J.H.M. Lange, Kraton Chemical B.V., Transistorstraat 16, 1322 CE Almere, The Netherlands. Telephone: +31 (0)365462800. E-mail: jos.lange@kraton.com